KEK--93-10

JP9404110

KEK Report 93-10
November 1993
A

Slow Extraction System of the KEK-PS

Y. SHOJI, K. MARUTSUKA, T. TOYAMA and H. SATO

NATIONAL LABORATORY FOR
HIGH ENERGY PHYSICS

KEK Reports are available from:

Technical Information & Library
National Laboratory for High Energy Physics
1-1 Oho, Tsukuba-shi
Ibaraki-ken, 305
JAPAN

Phone: 0298-64-1171
Telex: 3652-534 (Domestic)
(0)3652-534 (International)
Fax: 0298-64-4604
Cable: KEK OHO
E-mail: LIBRARY@JPNKEKVX (Bitnet Address)
library@kekvax.kek.jp (Internet Address)

SLOW EXTRACTION SYSTEM OF THE KEK-PS

Y. Shoji, K. Marutsuka, T. Toyama and H. Sato

National Laboratory for High Energy Physics
1-1 Oho, Tsukuba-shi, Ibaraki-ken, 305, Japan

Abstract

Half-integer resonance extraction at $2\nu_H = 15$ has been utilized for the KEK 12-GeV Proton Synchrotron (KEK-PS). Performance of the slow extraction has been progressing recently. A slow beam extraction system was constructed for the newly build North Counter Hall. For the old East Counter Hall, the power rating of the slow extraction instruments was improved in connection with an elongation of the flat-top. The quality of the extracted beam (extraction efficiency, beam emittances and spill structure) has been systematically measured and improved by concentrated efforts. Further, a new variation of the extraction modes (deuteron beam extraction and lower energy beam extraction) has been achieved in order to contribute to the various fields of physical experiments. This report gives up-to-date descriptions of the slow extraction system of the KEK-PS.

I Introduction

The KEK 12-GeV PS is a cascade type accelerator which consists of a pre-injector, a 40MeV linac, a 500MeV booster synchrotron and a 12GeV main ring (MR) [1]. Half-integer resonance extraction from the MR started in 1977 [2]. Since then, the simultaneous sharing of slow extraction and an internal target (IT) [3] has been in operation. Parasitic fast extraction [4] started in 1978, and ceased operation in 1981. Up to the present, many studies concerning the slow extraction [5,6] have improved the performance. Especially over the past few years, almost all of the system was replaced by a new one and the operation has greatly changed. Figure 1 shows the present layout of the KEK-PS.

In June 1990, the highest beam intensity of 5×10^{12} ppp (particles per pulse) was recorded at the MR. To accept a higher intensity proton beam up to 10^{13} ppp, a new experimental hall (North Counter Hall) was constructed [7], because the existing East Counter Hall can not afford such an intense beam. At the same time, an extraction line for the North Counter Hall was constructed using one long straight section of the MR, which had previously been used for the fast extraction. This new extraction line, which was completed in summer 1990, and the existing line for the East Counter Hall is called EP2. Routine operation of EP1 started in June, 1991, with a beam intensity of 3×10^{12} ppp [8].

Almost at the same time, the duty factor of the MR was upgraded from 20% to 50%. The extraction time (spill length) for EP2 was elongated from 0.5 sec per cycle

to 2.0 sec per cycle, and the operation cycle from 2.6 s to 4.1 s [8,9]. Figure 2 shows the extraction elements for EP1 and EP2 distributed around the MR. The new elements for EP2 are basically the same as those for EP1, except for three magnetic septa, which have a larger heat tolerance. In October, 1990, the proton beam was successfully extracted to the East Counter Hall with a long spill length of about 2 s. After this success, extraction with the long spill length has become routine at the KEK-PS. At present, however, the spill length for the North Counter Hall is 1.5 s, shorter than that of EP2, due to the heat problem of the magnetic septa [10]. An upgraded septa will soon be ready to be installed there. The extraction time for the IT is the same as that of a slow extracted beam.

In response to increasing demands from high energy and nuclear physicists, the KEK-PS has begun to accelerate particles other than 12-GeV protons; polarized protons [11] and deuterons. A polarized proton beam was extracted with 3.5 GeV to EP2 and used for physics experiments from May, 1987, to July, 1988 [12]. The first deuteron beam was successfully accelerated to the top energy (5.6 GeV/u)[13] and extracted to the East Counter Hall in January, 1992. Deuteron beams were used for physics experiments with deuteron energies of 3, 3.5, 4 and 5GeV/u in April, 1992 [14] and 1, 2, 2.35, 2.7 and 3GeV/u in April, 1993. To obtain reference data, proton beam extraction was performed at energies of 3.5, 4 and 5GeV in May, 1992. The acceleration of these particles has extended the area of physics experiments at the KEK-PS.

In the following sections we try to explain all of features of slow extraction at the KEK-PS. In section II we give a general description of the MR of the KEK-PS. In section III we describe the hardwires of the extraction system, such as the magnets, power supplies, beam monitors and computer control system. In section IV we discuss the spill control system. The system used to cancel any longitudinal wake field is also discussed in this section. In section V we explain the up-to-date performance of the normal extraction of 12-GeV proton beam.

II KEK 12-GeV PS Main Ring

The main ring is a strong focusing separated function type synchrotron, consisting of 4 superperiods with 7 FODO unit cells.[1] Two of the 7 cells have a 5m long missing bend straight section. These long straight sections are used for an injection system, two slow extraction systems and an RF acceleration system. The average radius of the MR is 54 m. The beta functions and the dispersion function of one superperiod are shown in Fig.3.

One operation cycle is normally 4.1 seconds as shown in Fig.4. Nine pulses of 500MeV protons from the booster are injected into the MR during the injection period of 0.5 s long. The protons are accelerated to the top energy in 0.79 s, passing the phase transition at 5.3 GeV. The protons are slowly extracted during the 2.1 s long flat-top.

The power supply of the main ring magnets was upgraded in 1990 to improve the duty factor [9]. It consists of thyrister rectifiers, harmonic filter banks and a reactive power compensator [15]. Three separated rectifiers are used for bending magnets (Bend), horizontally focusing quadrupole magnets (Q_F) and vertically focusing quadrupole magnets (Q_D). The current of the quadrupole magnets must be tracked separately to the current of the bending magnets for precisely tuning the betatron oscillation frequency to perform the optimum beam acceleration. The repetitive control has been applied to suppress any deviation from the desired current pattern [16]. During the injection and acceleration the horizontal and vertical tunes are set at 7.12 and 7.21, respectively. The working area is in a triangle surrounded by three resonance lines, such as $\nu_H = 7$, $\nu_H - \nu_V = 0$ and $\nu_H + 3\nu_V = 29$ [17]. No resonance correction has been performed.

The natural chromaticities of the MR are $\xi_H = -8.5$ and $\xi_V = -8.7$ for the horizontal and vertical planes, respectively. However, at the top energy, due to the sextupole components from the saturation of the Bends [18], the chromaticities change to $\xi_H = -18.4$ and $\xi_V = -0.6$ if the sextupole magnets are not excited. For a chromaticity correction, sixteen correcting sextupole magnets are distributed around the MR [19]. Each magnet is 0.5m long and its maximum sextupole field is 150 T/m^2. Eight horizontal correcting sextupole magnets (Sex.F) are set at the short straight sections of 4F and 6F of each superperiod. They are connected in series to one pulsed power supply. The other eight magnets are vertical correcting sextupole magnets (Sex.D), and are set at the short straight sections of 4D and 6D of each superperiod. They are also connected in series to the other pulsed power supply.

A correcting dipole magnet system had been operated by DC mode and steered the beam only during the injection period [19]. The controller for the closed orbit distortion correction during acceleration was made temporary by a PC-9801 personal computer [20] for polarized beam acceleration. At the present, the system which was improved in 1987 is able to control the closed orbit during not only the injection period, but also during acceleration and flat top periods. The system consists of 28 horizontal dipoles and 28 vertical dipoles. Each of them is independently controlled by a VME computer system [21]. The vertical steering magnets are also used to adjust the extracted beam orbit.

Four RF cavities located at the IV-1F and IV-2F long straight sections accelerate the proton beam at a maximum voltage of 23 kV each. The RF frequency changes from 6.0 MHz at the injection energy to 7.9 MHz at the top energy of the MR for protons. For deuterons, the frequency range is from 4.0MHz to 7.9MHz [13].

III Extraction Elements

The extraction system is composed of extraction quadrupole magnets (EQ), an octupole magnet (OCT), four ripple compensation quadrupoles (RQ1, 2, 3 and 4), four bump magnets (Bump1, 2, 3 and 4), an electrostatic septum (ESS) and five magnetic septa (Sep.A, B, C, D and E). Figure 5 shows the detailed layout of the extraction

septa and extraction line monitors at EP1. The system of EP2 is basically the same as that of EP1. There are four single wire profile monitors (SWPM) along the extraction line, each being associated with a beam loss monitor (LM). In addition, secondary emission chambers (SEC), fluorescent screens (FS) and segmented wire ionization chambers (SWIC) are available for each beam line.

Quadrupoles, Octupole and Bump Magnets

The main parameters of the magnets, EQ, OCT, RQs and Bumps, are listed in Table I and II. EQ, OCT, RQ1, RQ2 and Bump1-4 are iron-core pulsed magnets. The cores are made of laminations of 0.35mm thick S-30 plates and the end plates of 10mm SUS304. At the positions of EQ, RQ1 and RQ2, bellows ducts are used as vacuum chambers in order to suppress eddy current losses. RQ3 and RQ4 are air-core quadrupole coils which surround ceramic vacuum ducts. Initially, RQ1 and RQ2 were made for EP1, and RQ3 and RQ4 for EP2. However, RQ3 and RQ4 are now used for the feed-back control of both EP1 and EP2, and RQ1 and RQ2 are used for the feed-forward control, as will be described in section V.

The main parameters of `power supplies of these magnets are listed in Table III. The power supplies for EQ, OCT, and Bumps are transistorized power supplies with 3-phase thyrister rectifiers.

Extraction Septa

The main parameters of the extraction septa are listed in Table IV. Figure 6 is a drawing of ESS. It consists of two 1.5m long septa, which are combined in one unit, but are connected to independent DC voltage power supplies. The septum itself is made of 0.1 mm tungsten wires with 1.25 mm spacing. Only two wires snapped off during these several years of EP2 running and one wire snapped off during the first year run of EP1. The cathode electrodes are smooth Ti plates. The septum wires are set to ground and a negative high voltage is applied to the cathode electrodes. The parameters of DC voltage source are listed in Table V. Although the intended electric field is 90kV/15mm, the ESS now works with 100-120kV/15mm, and with a dark current of less than 0.2mA. Above this electric field strength, the dark current between the septum and the cathode grows rapidly.

Sep.A and Sep.B are pulsed magnetic septa set in vacuum chambers. Figure 7 shows a drawing of Sep.B. Sep.A is similar to Sep.B except for the number of coil turns. The radial positions of these septa, ESS, Sep.A and Sep.B, are remotely adjustable from the Central Control Room (CCR). They are carefully adjusted to minimize the beam losses at these septa.

Sep.C, Sep.D and Sep.E are similar type pulsed magnetic septa set in air. A drawing of Sep.C is shown in Fig. 8. These three septa are connected in series to one current source. A heat problem of Sep.D and Sep.E was the most serious limit on the flat-top elongation. We have obtained a sufficient heat tolerance by minimizing

uncooled part of coils at the septa end . In Fig.9 the improved septum for EP2 is compared with the old-type septum [10]. The septa are 32 mm thick each and are made of 8 turn 3.2 mm thick coils. Each coil is insulated by 0.6 mm ceramic coats and cooled by water cooling pipes having an inner diameter of 2.3 mm for EP2 and 2 mm for EP1. There are 16 water cooling circuits for one septum. Sep.D and Sep.E work at a mean current of more than 3000 A, with a water pressure loss of 6 kg/cm^2 and a water flow of 16 *l* /min.

The parameters of the power supplies for the septum magnets are listed in Table VI. The power supplies for Sep.A,B and Sep.C,D,E are both thyrister regulated power supplies. A sufficient stability of 10^{-3} has been achieved at the flat-top, including both reproducibility and ripple, by adopting a ripple reduction system, as shown in Fig.10. This is a feed-back system to the thyrister regulation angles with narrow band-pass-filters of 50 and 100Hz. The reduction rate of the ripple components is 15 and 10dB for 50 and 100Hz, respectively. The ripple components of higher frequencies are suppressed by a passive filter. At the beginning of the beam extraction period, the VME computer outputs an almost step-type signal as a reference signal of the power supplies of Sep.C, D, E. The transient response of the septa, however, had a ringing behavior. To remove this ringing, a reference signal produced by a VME computer was modified to compensate for, such a transient response at the start of the flat-top.

Monitors

There are two beam loss monitor (LM) systems. One is the MR loss monitor system. It consists of 56 gas-filled coaxial cables distributed around the MR, one cable for each half unit cell [22]. Each cable works as an ionization chamber. The integrated beam loss from the injection to any timing is displayed, and this is used for tuning the machine operation.

Another is located in the slow extraction line as shown in Fig.5 in order to tune the extracted beam direction. It consists of gas-filled tubes set at the upstream ends of ESS, Sep.A, Sep.B and Sep.C. Real time beam losses are monitored by an oscilloscope, one channel for one tube.

There are several kinds of beam profile monitors. A single wire profile monitor (SWPM) is a slowly movable wire across the extraction line, each being associated with a loss monitor. Figure 11 shows the principle of the SWPM. Three wires are set at the upstream ends of ESS, Sep.A and Sep.C to measure the horizontal beam profile of EP2; 8 wires, 4 for horizontal and the other 4 for vertical, are set at the upstream ends of ESS, Sep.A , Sep.B and Sep.C of EP1.

Along each beam line downstream of Sep.E, fluorescent screens (FS) and segmented wire ion chambers (SWIC)[23] are used as beam profile monitors.

The extracted beam intensity is normally measured with Secondary Emission Chambers (SEC), which are calibrated using the ^{27}Al (p, spallation) ^{27}Be reaction [24]. The calibration was made after every long shut-down (two times a year) and after each energy run, but it has been made recently once per one operation cycle to

make clear the extraction efficiency. The sum of systematic errors in the calibration amounts to about 10%. One of the SECs of each line is used as a spill-ripple monitor. The time constant determined by the SEC and an accompanied preamplifier is 0.05 ms; this is comparable to the frequency range of RQ systems. Figure 12 shows the gain curves of each SEC versus the bias voltage. SEC in the EP2 line has been used for the past decade, and its sensitivity has degraded. The intensity of circulating beam is measured with an active current transformer set in the MR [25]. The scintillation counter for the external target is utilized to monitor the high frequency component of several MHz in the spill ripple.

Computer Control System

Figure 13 shows the diagram of the computer control system for the extraction elements, replaced from the old computer system also in summer 1990. VME crates are set at the auxiliary power supply rooms (M3, A47 and nM2 in Fig.1) and at the CCR. All of the crates and graphic consoles are connected to the VME-bus MAP system [26]. There are many boards for digital delay, DAC, relay, digital input and ADC in VME crates. The digital delay boards set the extraction timings, the DAC boards produce reference pattern signals of magnet excitations, the relay boards control ON/OFF and RESET of power supplies, the digital input boards and ADC boards monitor the status signals of power supplies. These are controlled by touch-panels or key boards distributed in the CCR.

Radiation safety signals are sent to the power supplies of Sep.A,B and Sep.C,D,E by hard-wired lines that are independent of the VME computer system for security purposes in the experimental area.[27].

IV Spill Control System

In physics experiments the trigger rate or the counting rate of the data acquisition system is limited by the hardware and/or software architectures. In some cases detectors cannot separate multiple events, due to collisions with too many spilled particles and the target. In other cases, the data acquisition efficiency can be bad due to a large dead time when too much beam is extracted. Therefore, the spilled beam should be weak sufficiently so that almost all events are accepted by the data acquisition system. On the other hand, the spilled beam should be intense sufficiently so that the length of an experiment period is acceptable.

To compromise this occasion and to use the beam efficiently, one requirement for the slow extraction systems is a constant spill length with full utilization of the flat-top period. Since the spill length would change due to the cycle-to-cycle beam intensity variation for several reasons, if the extraction rate was constant, i.e. $\frac{dv_x}{dt}$ = constant, the extraction process should be adequately controlled.

The other requirement is a uniform intensity spill, i.e. a DC spill. In practice the spill has a time structure which is raised by any ripple of the magnet power supply and the rebunching of coasting beam. At the crest of the spill fluctuation, multiple events and/or a large dead time may occur in the data acquisition system of the physics experiments. Therefore, the control system is necessary to suppress the spill structure.

To realize the constant-time-length spill and to suppress the spill structure so as to be less than a few kHz due to the ripple of the magnet power supply, a feedback control system have been utilized. In this system the beam intensity signal is used as a reference signal to deal with the cycle-to-cycle variation, and the feedback loop suppresses the low frequency spill structure by changing the horizontal betatron tune via EQ and RQs. In addition, two feedforward loops and one feedback loop are newly installed in the spill control system and in the rf control system, respectively.

Efforts have also been continued to clear up and remove any causes which prevent the constant-time-length DC spill. The ripple of the main ring magnet current has been reduced by several methods. These subjects are described in references [15,28].

Feedback Control

The simplified feedback control system is shown in Fig.14. The extracted beam intensity signal (I_{SPILL}) from the SEC is compared with the reference level (N_0), which is proportional to the circulating beam intensity just before extraction. The error signal (N_0–I_{SPILL}) is integrated, applied phase-compensation and fed to two loops: EQ and RQs loops. EQ and RQs adjust the tune to correct any error. The transfer function of this part is summarized as $G_1(s)$ in Fig.14 We consider an external tune disturbance, d, which enters at the point A. The spill intensity is proportional to the tune change in time:

$$I_{SPILL}(t) \approx \frac{dN(\nu_H)}{d\nu_H} \cdot \frac{d\nu_H}{dt},$$

where I_{SPILL} is the spill intensity and dN is the particle number whose horizontal tune is $\nu_H \sim \nu_H + d\nu_H$. The transfer function of the slow extraction process is obtained by a Fourier transformation of the above equation:

$$G2(s) = \frac{I_{SPILL}(s)}{\nu_H(s)} \approx \left(\frac{dN(\nu_H)}{d\nu_H} \; s \right),$$

which has a different gain for a different density in the phase space.

With the feedback, the spill intensity due to N_0 and d acting simultaneously is

$$I_{SPILL} = \frac{G_1 \cdot G_2}{1+G_1 \cdot G_2} N_0 + \frac{G_2}{1+G_1 \cdot G_2} d.$$

A smaller error N_0–I_{SPILL} is achieved for a larger loop gain, $|G_1 \cdot G_2|$. On the other hand, the disturbance is eliminated for a larger $|G_1|$.

The schematic diagram of the circuit is presented in Fig.15. The loop via EQ keeps the spill length always constant and suppresses any intensity fluctuation in the

frequency range from DC to several hundreds hertz, while the loop via RQs (RQ3 and RQ4) suppresses any frequency components higher than several hundreds hertz [29].

In general a feedback loop gain is restricted by the stability of a control system. Therefore, in the spill control system the gain, $|G_1|$, should be set just below where the system becomes unstable since $|G_1|$ depends on the extraction process.

From the viewpoint of reducing the disturbance, a much higher gain, $|G_1|$, is required. To improve the characteristics of the spill control system, the frequency responses of the components are measured as follows. The frequency response of the EQ is shown in Fig.16. This indicates that the EQ's characteristic can be described by a second-order lag function except a large phase lag. This large phase lag is considered to be responsible for restricting of the phase margin of the servo-spill control. On the other hand, frequency response of the RQ is quite well up to 10 kHz as shown in Fig.17. Frequency response of the bellows ducts inside the EQ is almost flat at frequencies less than 10kHz in both gain and phase characteristics as shown in Fig.18. Therefore, an adequate phase-lead compensation will improve the characteristics of the spill control system. A detailed analysis of the present control system is given in references [30].

Feedforward Control

The performance of the feedback control is limited by the system stability, whereas feedforward control is the free from any instability of the control system. We added a feedforward loop in the spill control system to suppress any ripple effects much more efficiently. The main origin of a spill intensity fluctuation less than a few kHz is a fluctuation of the horizontal tune due to the QF ripple current. We canceled the tune fluctuation by feeding the inverted signal of the QF ripple to EQ or RQs in addition to the feedback signal. We tried two cases, one is the feed to EQ and another is the feed to the iron-core RQs.

The ripple signal measured by a search coil in a dummy magnet is inverted, amplified and fed to EQ of EP2. The amplifier gain is adjusted to minimize the 50Hz component of the spill ripple of EP2. No phase lag nor integration was applied. The 50 Hz component is reduced by a factor of *10*, which is comparable to the *limit* from a resolution of the adjustment. Also, the reduction of a continuum from 20 to 100Hz is observed. Especially, the broad peak at 75Hz has disappeared. At this frequency the noise reduction of the main power supply by the passive filter is smaller than that of 50Hz or 100Hz. The parameters are easy to be adjusted because they can be optimized independent to the parameters of the feedback system [29].

The same ripple signal of QF is fed to EQ of EP1, to minimize the 50 Hz component of the spill ripple of EP1. In this case, to obtain the reduction of 50 Hz component by a factor of 10, an additional phase lag of about 20 degrees is required.

On the other hand we have also made a trial in which the same ripple signal is inverted, amplified, integrated and fed to iron-core RQs (RQ1 and RQ2), because the air-core RQs (RQ3 and RQ4) cannot produce a sufficiently strong quadrupole field.

That reduces the higher frequency components from 100Hz to 1kHz by 5dB-20dB.[29] The phase was fixed to a suitable value. The optimum gain of the amplifier was a little bit different for each frequency component from 150 Hz to 600 Hz.

A few dB variation of the spill ripple was observed within a day. This variation can be automatically corrected by the repetitive control method[16].

Forward controller to improve the transient response

The spill control system has an overshoot in the step response. As the reference signal of the spill control system is nearly a step function, the obtained spill signal has an overshoot which is larger for a larger loop gain. This corresponds to the peak at a few hundred Herz in the gain curve of the closed-loop frequency characteristic. This overshoot should be avoided during the physics experiments. This can be compensated by a sort of forward controller.

A forward-compensation scheme is, in principle, as follows. Assume a certain system whose transfer function can be written as H(s), the output of the system, Y(s), is

$$Y(s) = H(s)\ \frac{1}{s}$$

without any compensation, where s is the Laplace operator and the step function $\frac{1}{s}$ is assumed as the input of the system. If one can prepare the forward controller as $H^{-1}(s)$ or use the input $X'(s) = H^{-1}(s)\ \frac{1}{s}$, it is possible to obtain an ideal step response as

$$Y(s) = H(s)\ H^{-1}(s)\ \frac{1}{s} = \frac{1}{s}\ .$$

In reality, we can only use an approximate form of $H^{-1}(s)$.

In the spill control system, an optional short trapezoid pulse (corresponds to X'(s)) is added to the EQ pattern at the beginning of the spill [29]. The optimized shape of the trapezoid depends on the characteristics of the feedback loop: the loop gain variation due to the beam intensity, particle distribution in phase space etc. It is then adjusted at every extraction tuning. To tune the shape of the trapezoid automatically, a possible method may be the repetitive control method [16].

Rebunch Suppression

To suppress the re-bunching phenomenon, the bunch signal of the circulating beam was fed to the RF cavity during extraction.[29] Two main frequency components growing in the coasting beam are 7th and 8th harmonics of the revolution frequency, since the resonant frequency of the RF cavity is detuned to about 6.4MHz, that is 7.3 times the revolution frequency. The phase of both components are adjusted with the delay time of one period of RF to minimize these components. The signal was amplified and fed to one of four RF power amplifiers.

V Operation Summary of Extraction

The sequence for the beam extraction tuning: rf off, magnet on, tune shift and so on: is very important to achieve stable operation, as well as adequate settings of the parameters. In this section the practical beam extraction procedure is briefly described in connection with the behavior of the extraction equipment and the beam dynamics.

Extraction Cycle

The slow beam extraction is carried out according to the timing chart shown in Fig.19. Just after reaching the top energy, the horizontal closed orbit displacement due to momentum displacement is changed to an adequate extraction orbit by RF acceleration or deceleration, since this parameter is kept at an optimum value for the efficient phase transition passing up to the top energy. To debunch the beam, twenty msec after that, the RF voltage is decreased to zero in less than 0.2 ms, much smaller than the synchrotron oscillation frequency (380Hz). At the same time the resonant frequency of the RF cavities is detuned to about 6.4 MHz for the rebunch suppression described above.

After the beam is debunched, the horizontal betatron tune, ν_H, is changed from 7.12 to 7.40 within 40 ms by increasing the field gradient of the Q_F by about 3%, while the vertical tune, ν_V, is kept constant at 7.21. The transient response of the Q_F current due to this tune shift settles down within 100 ms after starting the tune shift. Magnetic fields of the septa, OCT and bump magnets are increased to the set value by this time.

Extraction starts when an extraction start signal opens the gate for the controller in the feedback control circuits. The EQ and RQs are excited according to the feedback signal. During extraction, Q_F current is linearly increased at a rate of about 0.5%/2s in order to keep the EQ current roughly constant. Otherwise, increasing the EQ current cause an increasing deformation of the β function and would cause the larger horizontal orbit displacement of extracted beam [31]. The shape of the EQ current pattern reflects the horizontal tune variation during extraction, depending on chromaticity, momentum distribution and so on.

The local bump orbit for extraction is created by four bump magnets. The positions of the bump magnets and the typical bump orbit are shown in Fig.20. This system can create a local bump at the entrance of ESS: 0~30 mm for an orbit displacement and 0 ~ − 4 mrad for a gradient. Because of the negative horizontal chromaticity, the lower momentum particles are extracted at first. The closed orbit of the extracted particle is the inner side of the ring at the extraction start, due to the finite momentum dispersion of about 2 m at the ESS entrance. Toward the extraction end the closed orbit shifts the outer side. The closed orbit displacement is $\pm$ 8 mm for $\Delta p/p = \pm$ 0.4 %. Therefore, the local bump orbit is changed during extraction, decreasing from the extraction start to the extraction end. The calculation shows that this bump variation is available by using the present bump system. However, the experiment shows that the turn separation decreases from the extraction start to the extraction end, even after appropriate bump

tuning. This seems to indicate the lack of a bump capability. This inconsistency shoud be solved by future study.

Operating Point

The operating point on the tune diagram moves during the extraction process as shown in Fig.21. As described above, the vertical tune, ν_V, is kept at nearly 7.2, which is of the smallest beam loss. This vertical tune is selected based on the result of an extensive survey of the tune diagram at the injection period. Some of the results are shown in Fig.22. Along the line, $\nu_H = 7.4$, there are two areas of beam survival at around $\nu_V = 7.2$ and 7.44. When the operating point moves from (ν_H, ν_V)= (7.21, 7.12) to (7.4, 7.44), it must pass more resonances. The area near to the $\nu_V = 7.2$ point is then selected for extraction.

The measured vertical tune dependence on the extracted beam profile indicates the blow-up of the vertical beam size near to $\nu_V = 7.25$. Just below this operation point the vertical profile of the extracted beam has a very curious (two peaks and no blow-up) shape [32]. There is no meaningful change of the extracted beam in the region from $\nu_V = 7.1$ to $\nu_V = 7.2$.

Parameters of the Extracted Beam

The horizontal beam size at the small dispersion position, measured by nondistractive profile monitor (NDPM) at I-3F, is almost constant during the extraction, and that at the large dispersion position, measured by NDPM at IV-5F, decreases from the inner side of the ring [33]. This means that the beam is extracted from the lower momentum component to the higher momentum component. This is consistent with the result of the measured momentum spread as a parameter of the sextupole field strength[6]. The horizontal chromaticity is roughly set at the natural chromaticity, and the variation of the Qf current during the extraction corresponds to the momentum spread of 0.6%-0.8%.

The typical horizontal trajectory through the extraction septa is shown in Fig.23. The horizontal aperture for the circulating beam is narrowest at the entrance of Sep.C. This is because the aperture of QF is shared with the circulating beam, the extracted beam and the space for the thick septum (Sep.C). Beyond the region of $\pm$80mm, the quadrupole component of QF is less than 90% to that at the magnet center.

The vertical aperture through the septa is 16 πmm·mrad as shown in Fig.24. It is sufficient for the 12-GeV extraction. However, for a lower energy beam extraction than 1 GeV, even if the vertical emittance damps adiabatically, the emittance exceeds the aperture of the extraction line. Then, a part of the beam should hit the septum yoke and be lost.

The sum of the outputs of 56 MR loss monitors indicates a beam loss of 3% during the extraction of EP2. That is, the beam loss at the ESS and Sep. A is ~ 1.4%, the beam loss at the Sep. C, D and E is less than 0.7% and the beam loss distributed

around the ring is ~ 0.9%. In the case of simultaneously using the IT, an additional beam loss corresponding to 0.5% of the circulating beam is observed around the IT. On the other hand, the beam loss for EP1 is about 6%, worse than that of EP2. In this case beam losses at the Sep.B and II-4F section are observed. At the corresponding positions of EP2, we observe beam losses of less than EP1. About 1.4% loss at the ESS and Septum A is a reasonable value compared with the probability of hitting the septum. This is because many of the particles are lost at downstream of the ESS and Sep.A.

VI Conclusion

The slow extraction system of the KEK-PS at the present has been described. A long spill length slow beam extraction to the renewed EP2 line and the new EP1 line has been successfully performed with good reliability. The uniformity of the spill has been improved due to several efforts. However, the dynamics of the extraction process coupled with the servo-spill control system does not seem to be clear, which depends on the transverse betatron tune variation during extraction, chromaticity, momentum distribution and so on. It is necessary to continue the investigation of these effects and dynamics to clarify the extraction process and to make a flexible servo-spill control system.

A study about the extraction of low momentum particles has just started. The extracted beam profile highly depends on the value of chromaticity when the protons or deuterons are extracted at the momentum lower than 9 GeV. These things concerning beam dynamics are still under investigation.

Acknowledgment

The authors thank professor N. Kumagai for his contribution to earlier parts of this work. We are grateful to S. Ninomiya and M. Yoshii for their help in rebunch suppressing, to the crew of the beam channel group of the KEK-PS for their helpful advice and the preparation of some data concerning the extracted beam, to members of the control group for their preparation of the computer system and to the monitor group of the KEK-PS and professor Kawakubo and H. Nakagawa for their help in taking some data.

We also thank for professor M. Kihara for his support, encouragement and especially careful reading and discussion of this report.

References

[1] T. Suzuki, KEK-74-4.
[2] E. Endo and C. Steinback, KEK-77-13.
[3] C. Steinback and K. Endo, KEK-77-18.
[4] J. D. McCarthy and Y. Kimura, KEK-74-16.

[5] K. Endo et al., Proc. of Particle Accelerator Conference, 1979, San Francisco, IEEE Trans. on Nucl. Sci., vol. NS-26, No.3, p.3170.
[6] S. Ninomiya et al., Proc. of the 6th International Conf. on High Energy Accelerators, 1980, Geneva, Switzerland, p.341.
[7] K. H. Tanaka, Proc. of the Workshop on Science at the Kaon Factory, Vancouver, Canada, 1990, p.1.
[8] Y. Shoji et al., Proc. of the 8th Symp. on Accelerator Science and Technology, 1991, Saitama, Japan, p.281.
[9] H. Sato et al., Proc. of the 1991 IEEE Particle Accelerator Conference, San Francisco, 1991, p.908.
[10] K. Marutsuka, KEK Accelerator Internal, OB-116(1992).
[11] H. Sato et al., Nucl. Instr. & Meth. A272 (1988) 617.
H. Sato, Jpn. J. of Appl. Phys., 27(1988)102.
[12] C.Ohmori et al., Physics Letters B243(1990)29.
H.Shimizu et al., Phys.Rev.C42(1990)R483.
[13] Y.Mori et al., Proc. of the 8th Symp. on Accelerator Science and Technology, 1991, Saitama, Japan, p.7.
[14] J.Chiba et al., Nucl. Phys. A553(1993)771c.
[15] H. Sato et al., IEEE Trans. NS39(1992)1490.
[16] T.Sueno et al.,Proc. of the 14th Int. Conf. on High Energy Accelerators, 1989, Tsukuba, Japan, Particle Acc. 29(1990)133.
[17] Y. Shoji et al., KEK Accelerator Internal SR-279(1992).
[18] T. Kasuga et al., Proc. of 5th International Conf. on Magnet Technology, 1975, Frascati, p.74.
A. Ando et al., Proc. of the 9th International Conf. on High Energy Accelerators, 1974, Stanford, p.610.
[19] A. Ando et al., Proc. of 5th International Conf. on Magnet Technology, 1975, Frascati, p.63.
[20] H.Sato, S.Hiramatsu, S.Ninomiya and D.Arakawa, Proc. of the 4th Symp. on Acc. Sci. & Tech.(1982)147.
[21] Y. Shoji et al., Proc. of the 8th Symp. on Accelerator Science and Technology, 1991, Saitama, Japan, p.332.
[22] H. Nakagawa et al., Nucl. Instr. & Meth. 174 (1980) 401.
[23] K. H. Tanaka et al., Proc. of the Workshop on Advanced Beam Instrumentation, 1991, Tsukuba, Japan, p.145.
[24] M. Ieiri et al., Proc. of the 9th Symp. on Accelerator Science and Technology, 1993, Tsukuba, p.477.
[25] S.Hiramtsu et al., KEK-77-21
[26] T. Katoh et al., Proc. of the 14th International Conf. on High Energy Accelerators, 1989, Tsukuba, Japan, p.905.
[27] E. Kadokura et al., KEK Internal 90-21, Aug. 1990(in Japanese).
[28] H. Sato et al., Conference Record of the 1992 IEEE Nuclear Science Symp., 1992, Orland, Florida, p.569.

[29] Y. Shoji et al., Proc. of the Symp. on Accelerator Science and Technology,1991, Saitama, Japan, p. 329, .
H.Sato et al., Proc. of the 15th International Conference on High Energy Accelerator, Hamburg, Germany, 1992,p.495.
[30] H.Sato et al., Proc. of the 9th Symp. on Accelerator Science and Technology, 1993, Tsukuba, p.208.
T.Toyama et al., Proc. of the 9th Symp. on Accelerator Science and Technology, 1993, Tsukuba, p.404.
[31] N. Kumagai, KEK Accelerator Internal ASN-270(1987).
[32] Y. Shoji, KEK Accelerator Internal ASN-323(1992)(in Japanese).
[33] T. Kawakubo et al., Proc. of the International Conf. on Acc. and Large Exp. Phys. Cont. Systems, 1991, KEK, p399.

Table I Parameters of the extraction magnets. RQ1 and RQ2 are identical. RQ3 and RQ4 are the same type magnets. The core length and bore radius of RQ3 and 4 are the length and mean radius of air-core coils. The data concerning water cooling are bench test results.

magnets	EQ	OCT	RQ1, 2	RQ3, 4
weight (kg)	220	200	90	
gap (mm)	43.60	25.85	43.60	
core length (mm)	200	160	60	250
bore radius (mm)	62	80	62	80
coil turn (per pole)	22	18	24	14
resistance (mΩ)	38	52	55	84
inductance (mH)	5	8	1.5	0.38
maximum current (A)	500	500	30	30
maximum voltage (V)	60	60	200	30
max field (T/m, T/m^3)	7.21	1130	0.3	0.16
cooling water circuit	4	4	air	air
water press. (kg/cm^2)	10	10		
water press. loss	4	4		
water flow (l/min)	4	7		

Table II Parameters of the extraction bump magnets.
Bump magnets 2, 3 and 4 are identically the same type of magnet.

magnets	Bump1	Bump2,3,4
weight (kg)	200	460
pole gap (mm)	62	62
core length (mm)	170	430
gap width (mm)	200	200
coil turn (by pole)	42	42
resistance (mΩ)	40	60
inductance (mH)	7	17
maximum current (A)	250	250
maximum voltage (V)	55	55
max field (T)	0.21	0.21
cooling water circuit	2	2
pressure (kg/cm^2)	10	10
pressure loss (kg/cm^2)	5	5
water flow (l/min)	2.6	1.9

Table III Parameters of the current regulated power supplies for the extraction magnets. There are four types of power supplies, and one power supply for one magnet. The power supplies for the RQs are precision power amplifiers: 4520 (NF Electric Instrument Corp.). All power supplies are cooled by air.

	EQ, OCT	RQ1-4	Bump1	Bump2-4
width (mm)	1500	440	700	700
height (mm)	1800	510	1800	1800
depth (mm)	1000	690	900	900
max current (A)	500	15	250	250
max voltage (V)	60	±200	35	55
stability (%)	0.1	< 2	0.1	0.1
ripple (%)	0.01	20 mV	0.1	0.1
response	300 Hz	20 kHz	10ms	10ms
time lag(ms)	1, 0.8	-	8	8, 6, 4
source	400V 3ϕ	200V 1ϕ	200V 3ϕ	200V 3ϕ

Table IV Parameters of the extraction septa.

* The horizontal aperture is variable

** Height of Ti cathode. Yoke aperture is 100 mm

septum	ESS	Sep.A	Sep.B	Sep.C	Sep.D, E
thickness(mm)	0.1	1.0	2.0	16.0	32.0
coil turn		1	2	4	8
length(m)	1.5 X 2	0.9	0.7	1,5	1.3
field strength	6MV/m	0.08T	0.16T	0.8T	1.6T
hor. aperture (mm)	10-40*	62	47	91	75
ver. gap (mm)	50**	35	35	34	34
environment	vacuum	vac.	vac.	air	air
deflection angle(mrad)	1.4	1.6	2.5	28	49

Table V Parameters of the DC high voltage supply for the ESS.
(Nichicon DCG-200K3M)

maximum out put voltage	200	kV
limit current	3	mA
stability	< 1	% for AC source 100V ± 10%
ripple	< 1	% at 200kV 3mA operation
Source	AC 100V 50Hz 1	

Table VI Parameters of the current regulated power supply for the magnetic septum. Two septa, A and B, are connected in series to one power supply. Three septa, C, D and E, are connected in series to one power supply. Though the frame sizes are different for EP1 and EP2, the performance of the power supplies are the same.

	Sep.A,B	Sep.C,D,E
width EP1/EP2 (m)	3.3 /4.8	6.0 /7.5
height EP1/EP2 (m)	2.75/2.35	2.75/2.35
depth (m)	1.5	1.5
regulation current (A)	330-3300	600-6000
maximum voltage (V)	20	120
maximum power (kW)	66	720
reproducibility (%)	< ± 0.1	< ± 0.1
non-linearity (%)	< ± 0.1	< ± 0.1
ripple (%)	0.025	0.015
response time (ms)	10	10
Source	400V 3φ	400V 3φ
cooling	forced air	forced air

Table VI Parameters of the extracted beam (for 12 GeV protons)

	EP1	EP2	IT	unit
ε_x	4	4		πmmmrad
ε_z	3	3		πmmmrad
$\frac{\Delta p}{p}$	0.4	0.4		%
Intensity	$3\sim4\times10^{12}$	$3\sim4\times10^{12}$	$\sim1\times10^{11}$	ppp
Spill length	2000	1500		msec
Spill duty factor*)	~95	~95		%
Extraction efficiency	~99	~94		%

*) spill duty factor mentioned above is for the frequencies less than 1kHz.

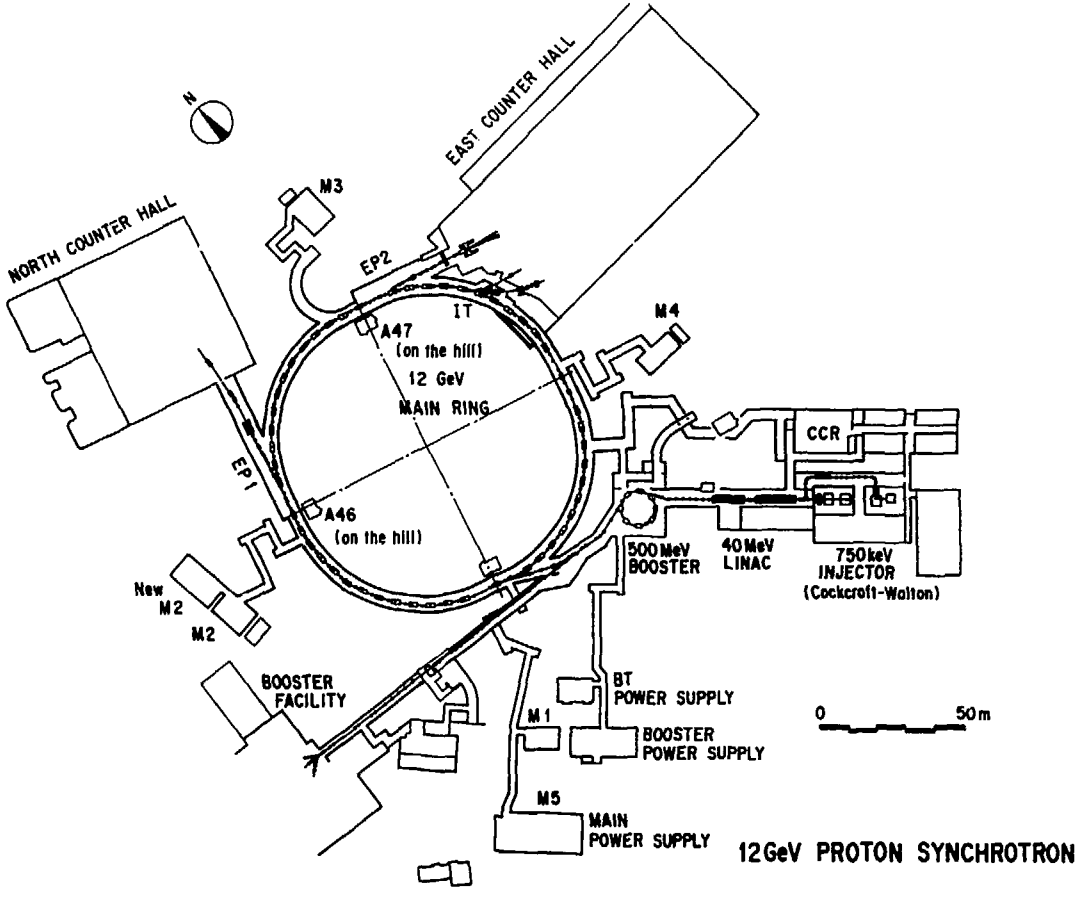

Fig.1 Lay out of the KEK-PS.

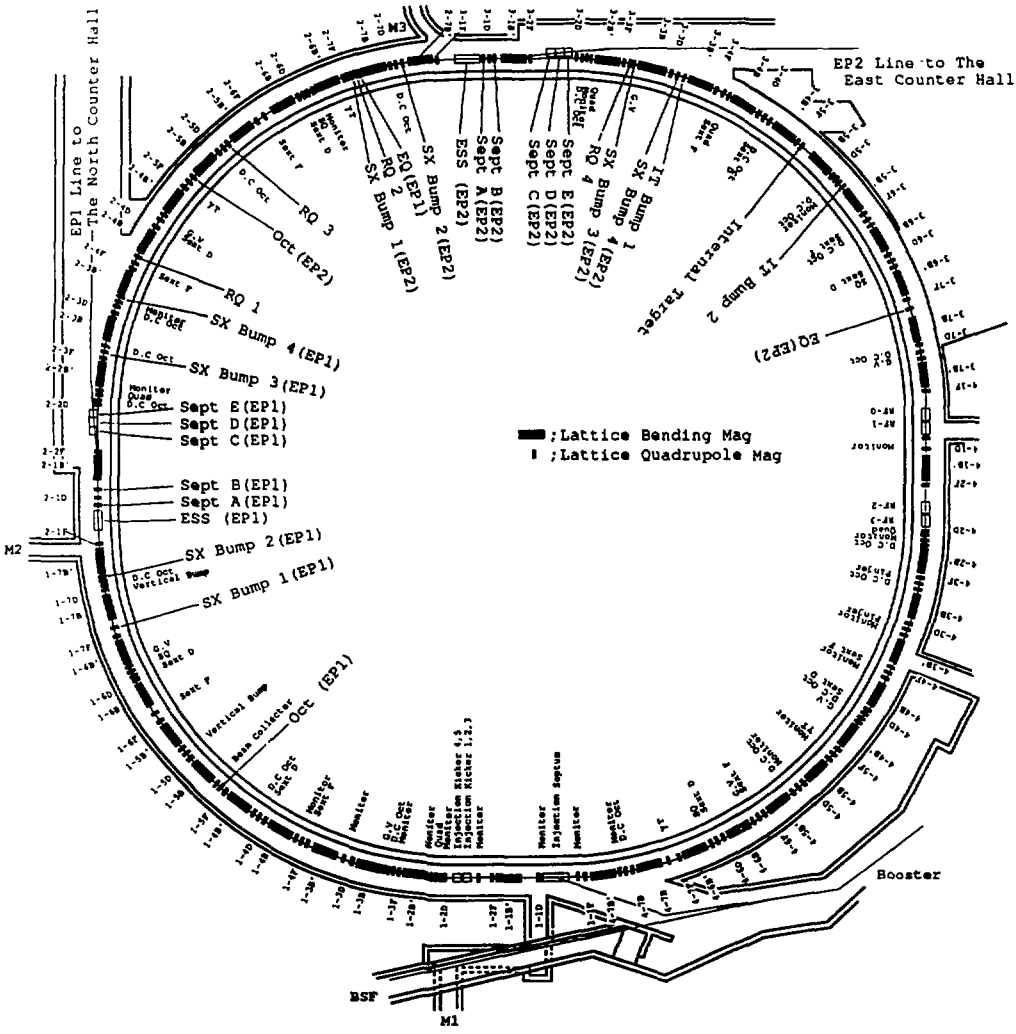

Fig.2 Extraction elements of the KEK-PS MR. Two sets of slow extraction system were installed during the summer 1990. Parameters of each elements are listed in the tables.

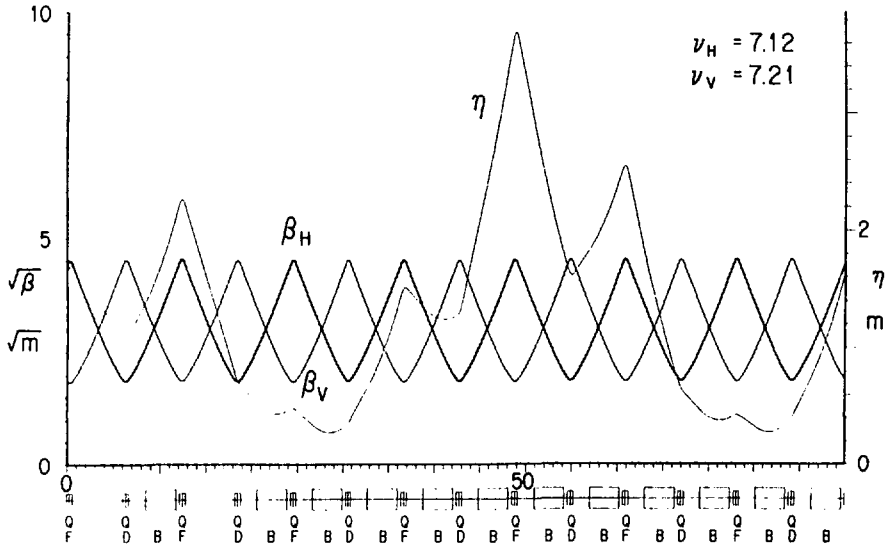

Fig.3 Beta functions and dispersion function of one super period of the MR of KEK-PS.

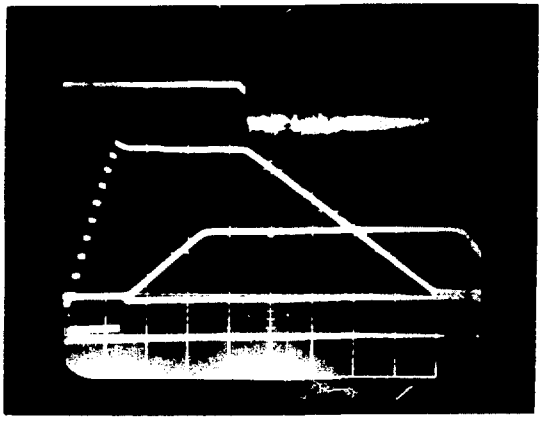

Fig.4 Normal operation cycle of the KEK-PS. One cycle is about 4.0 seconds. The top is the inverted intensity of the slow extracted beam. The second is the slow intensity of the circulating beam. The third is the current pattern of the lattice bending magnet. The fourth is the slow intensity of the Booster Synchrorton. The beam current of the Booster Synchrorton injected to the MR is lower than that into the Booster Synchrorton Facility.

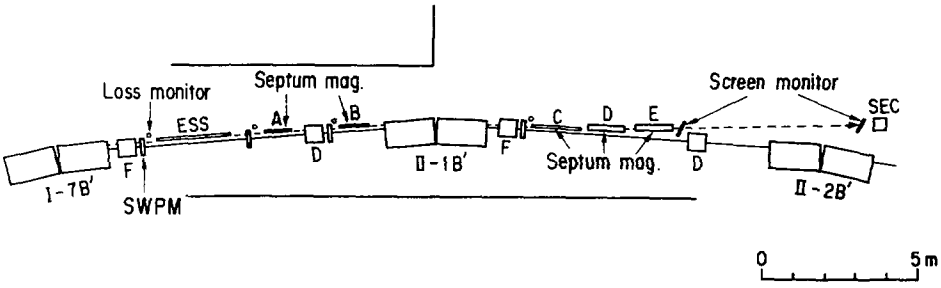

Fig.5 Layout of extraction septa and beam monitors of EP1. The layout of EP2 is basically the same as this. Beam runs in the vacuum from the MR to the II-2F and runs in the air from Sep.C.

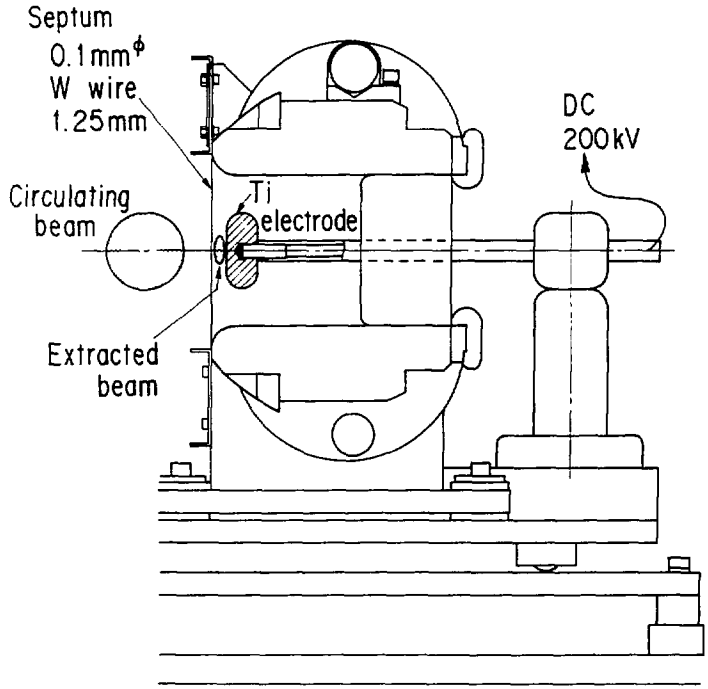

Fig.6 Structure of the Electro Static Septum (ESS).

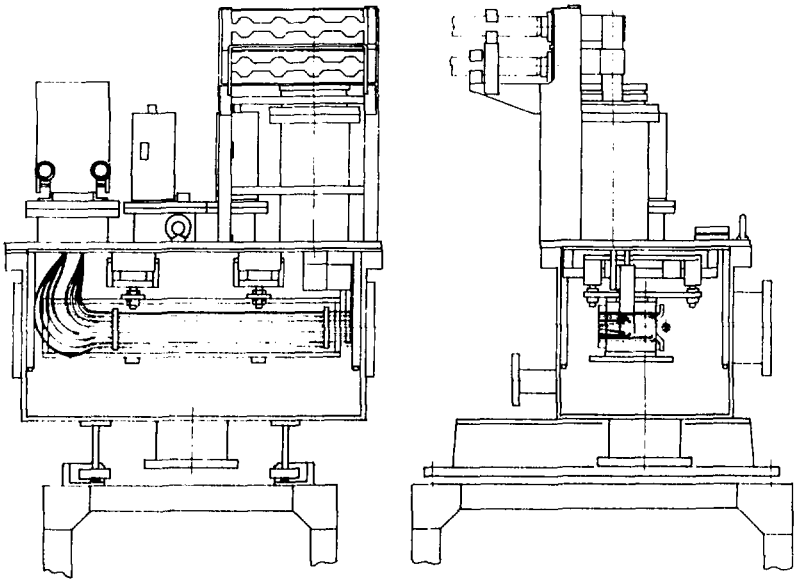

Fig.7 Structure of the Sep.B. Structure of the Sep.A is almost similar to that of the Sep.B except for the many coil turns. The septum structure is hanged from the top plate of the vacuum chamber.

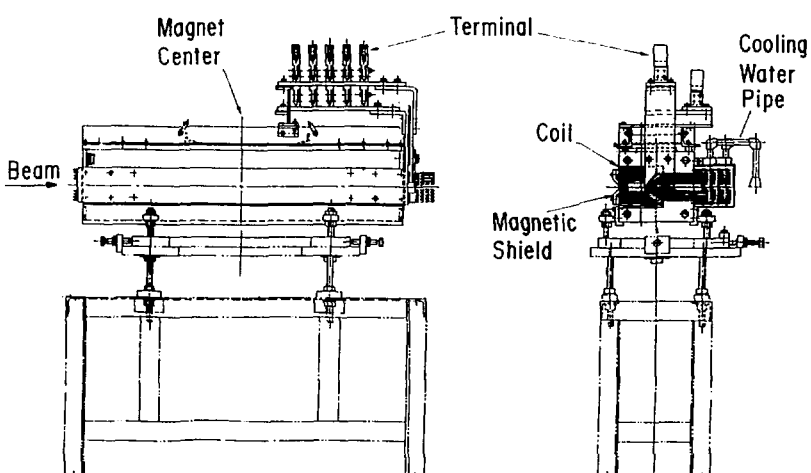

Fig.8 Structure of the Septum C. Structure of the septum D and E are almost similar to that of the Septum C. The positions of these septa are manually adjustable.

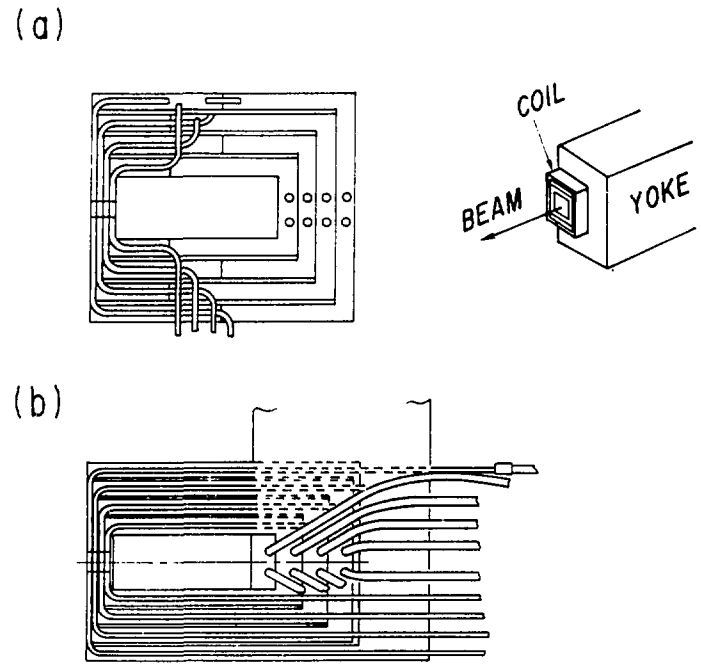

Fig.9 End structure of Septum C for (a) EP1 and (b) EP2. The water cooling pipes of EP2 septa pass through the end of conductors, those have therefore a large heat tolerance.

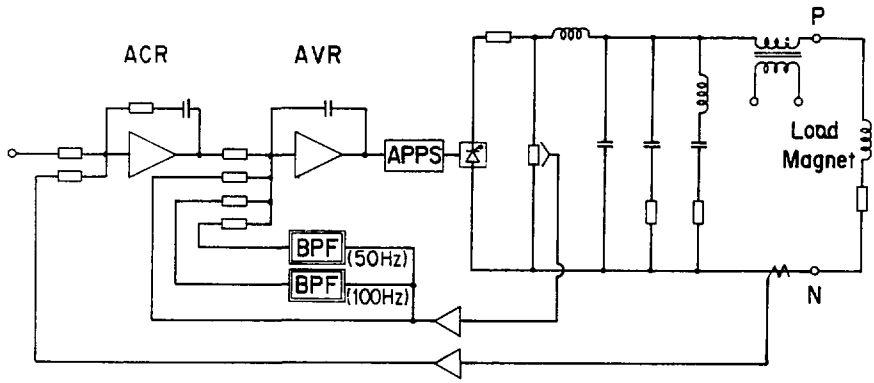

Fig.10 Ripple reduction system of the thyrister rectifier used in the power supplies of the magnetic septa. Two feed-back loops with narrow band pass filters suppress the 50 and 100 Hz ripple.

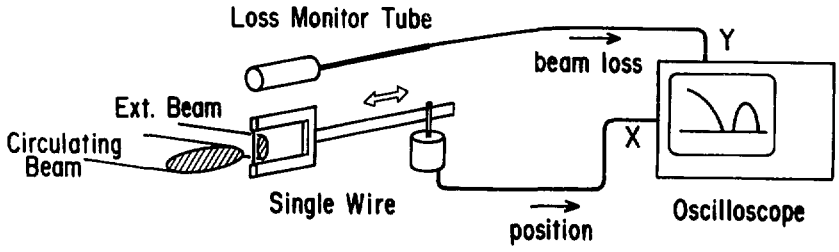

Fig.11 Principle of the Single Wire Profile Monitor. The oscilloscope displays the amount of beam loss versus the single wire position.

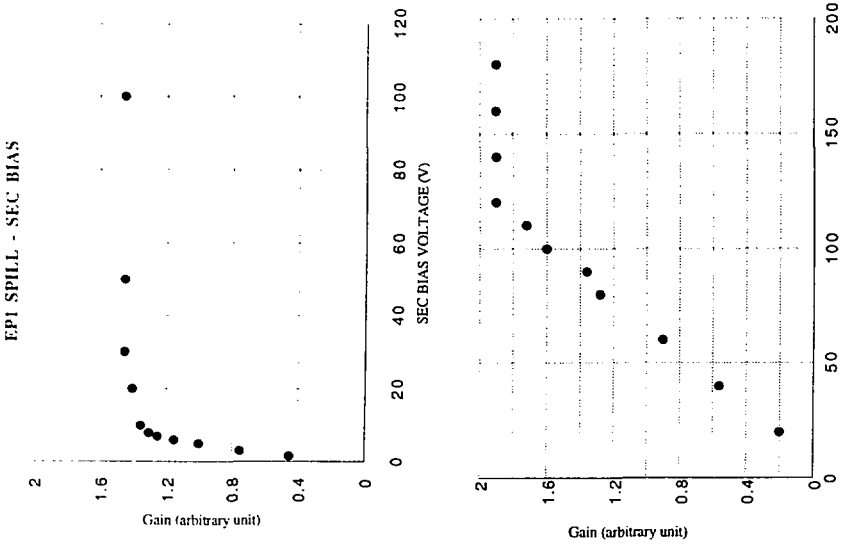

Fig. 12 Gain curve of SEC versus bias voltage.

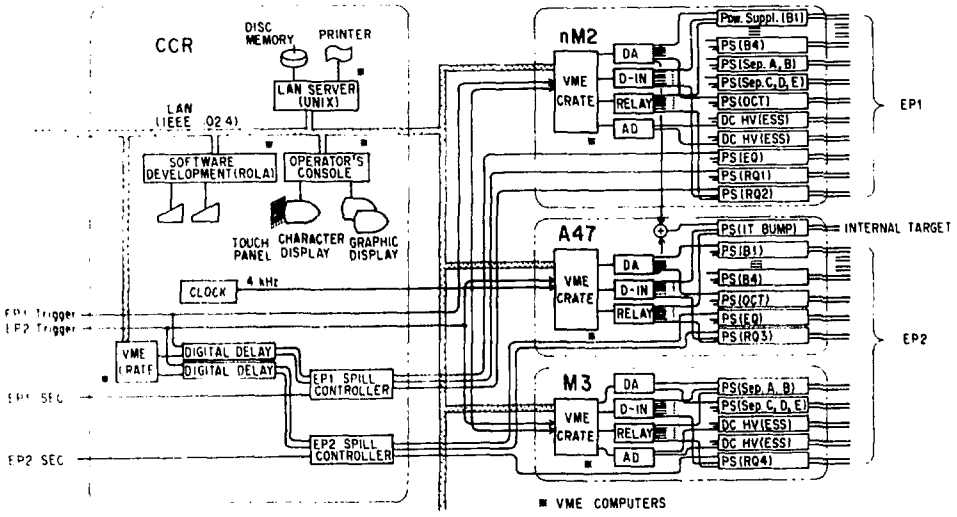

Fig.13 Computer control system of the extraction elements. The power supplies for the extraction magnets of EP1 are set auxiliary room nM2. Those of EP2 are set separately in two auxiliary rooms, M3 and A47. (cf. Fig.1)

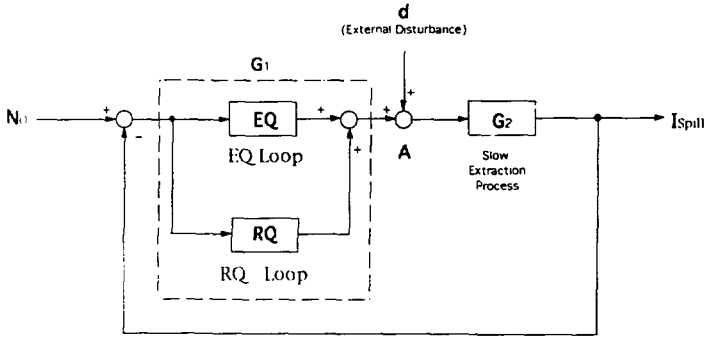

Fig.14 General description of the spill control system.

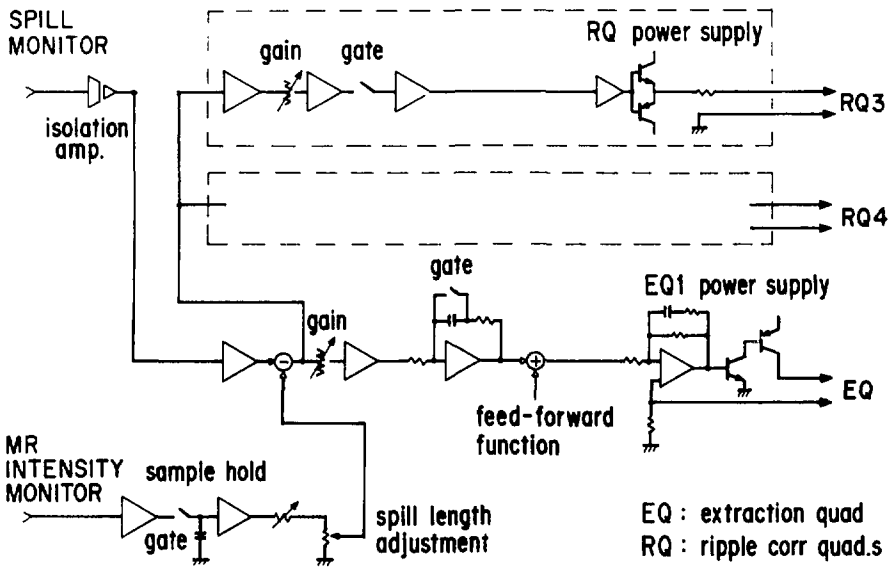

Fig.15 Schematic diagram of the circuit of the spill feed-back control.

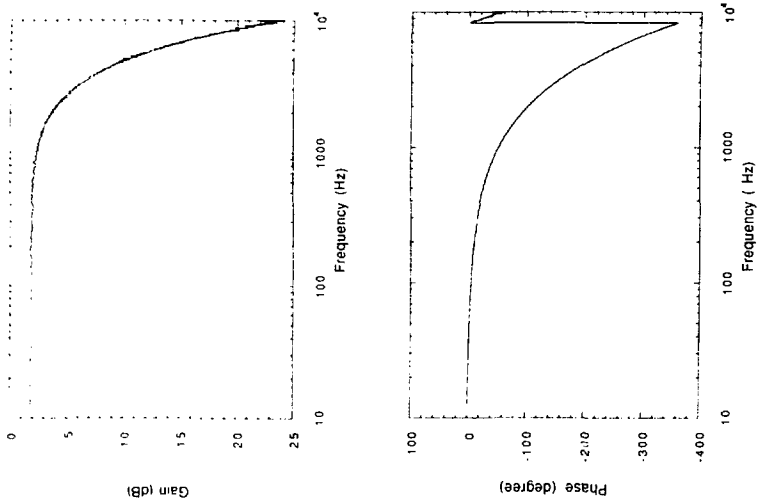

Fig.16 Frequency response of the EQ.

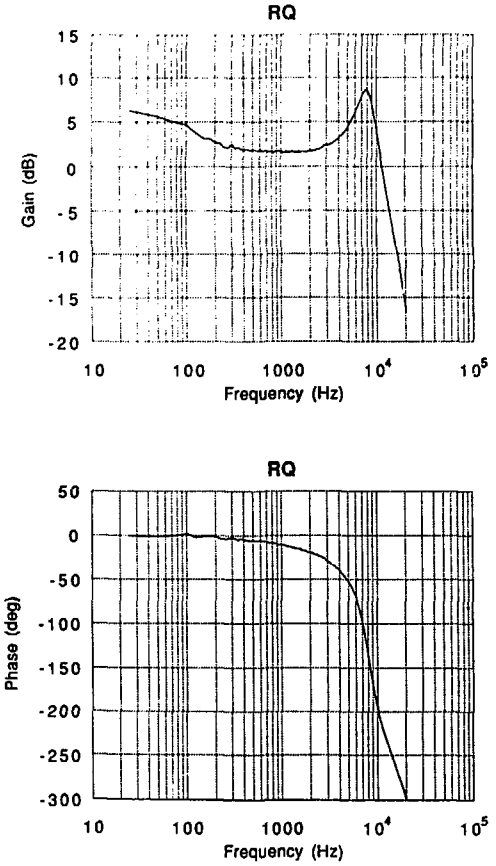

Fig.17 Frequency response of the RQ.

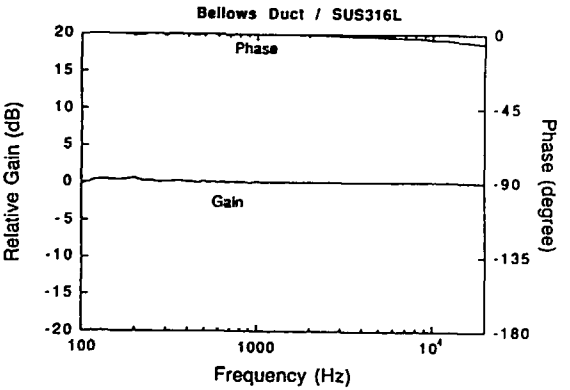

Fig. 18 Frequency response of the bellows ducts inside the EQ.

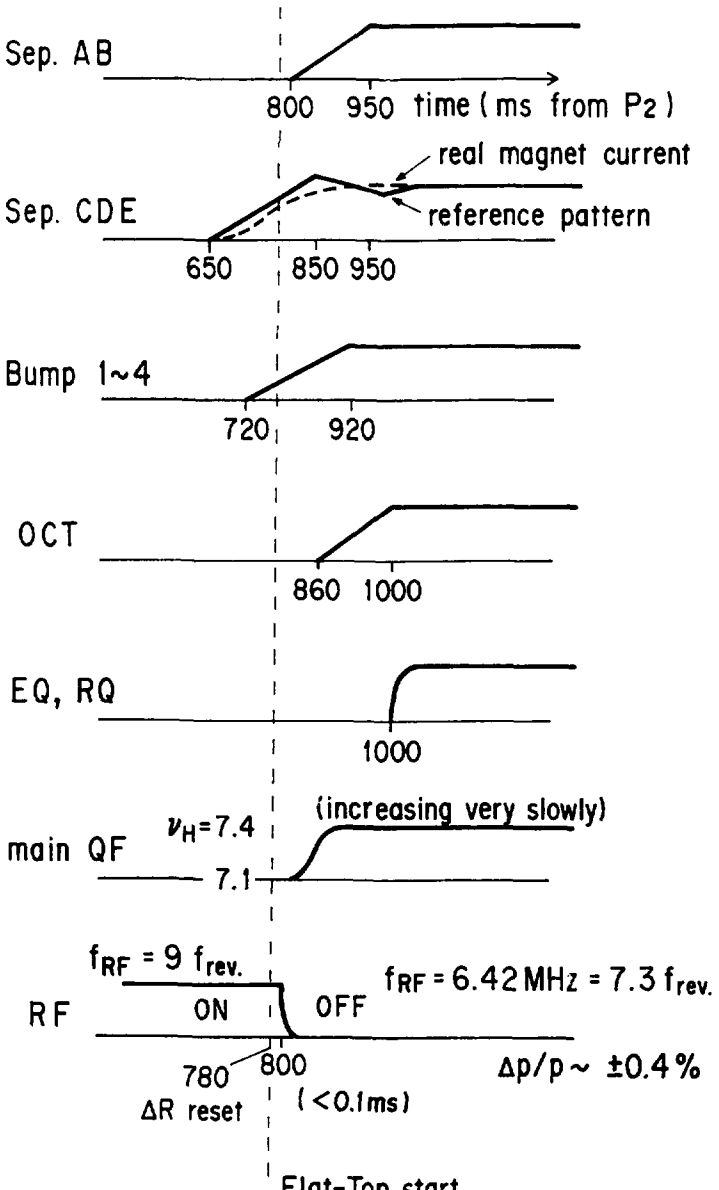

Fig.19 Timing table of slow extraction for the EP2.

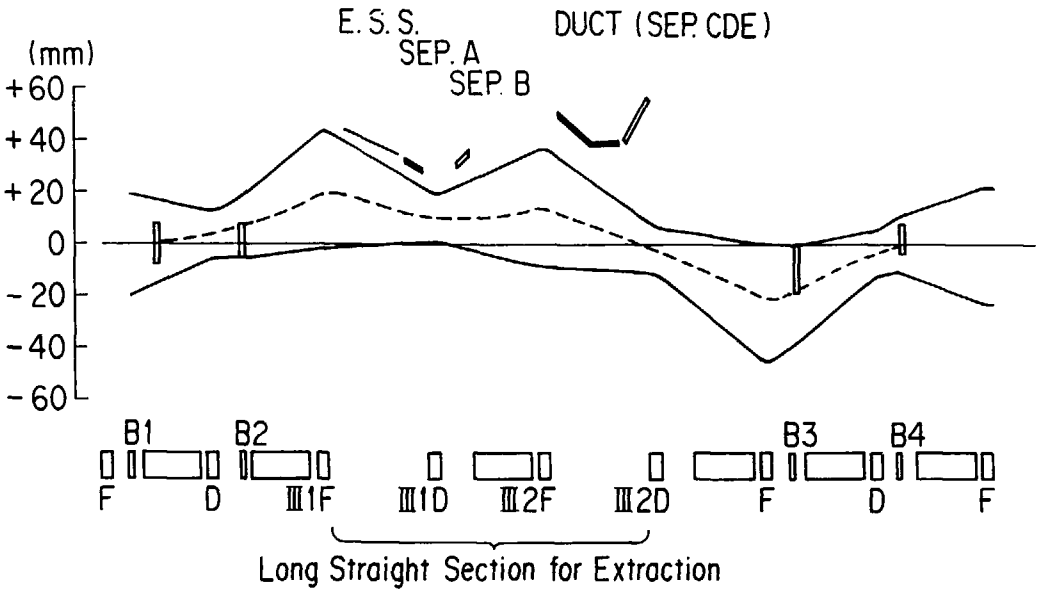

Fig.20 Position of the four extraction bump magnets of EP2 and a typical bump orbit.

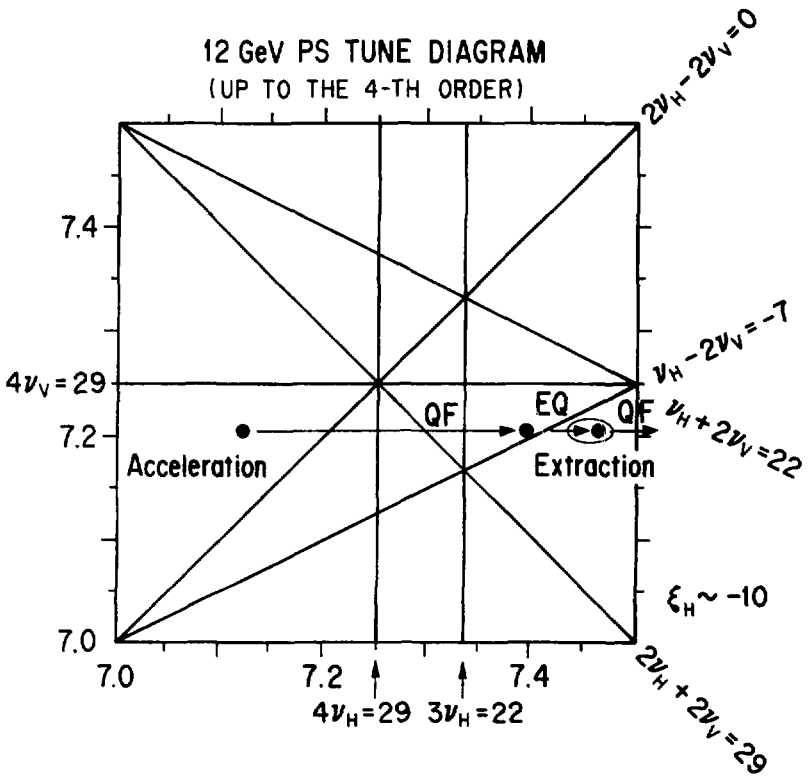

Fig.21 Tune diagram and operating point of the KEK-PS.

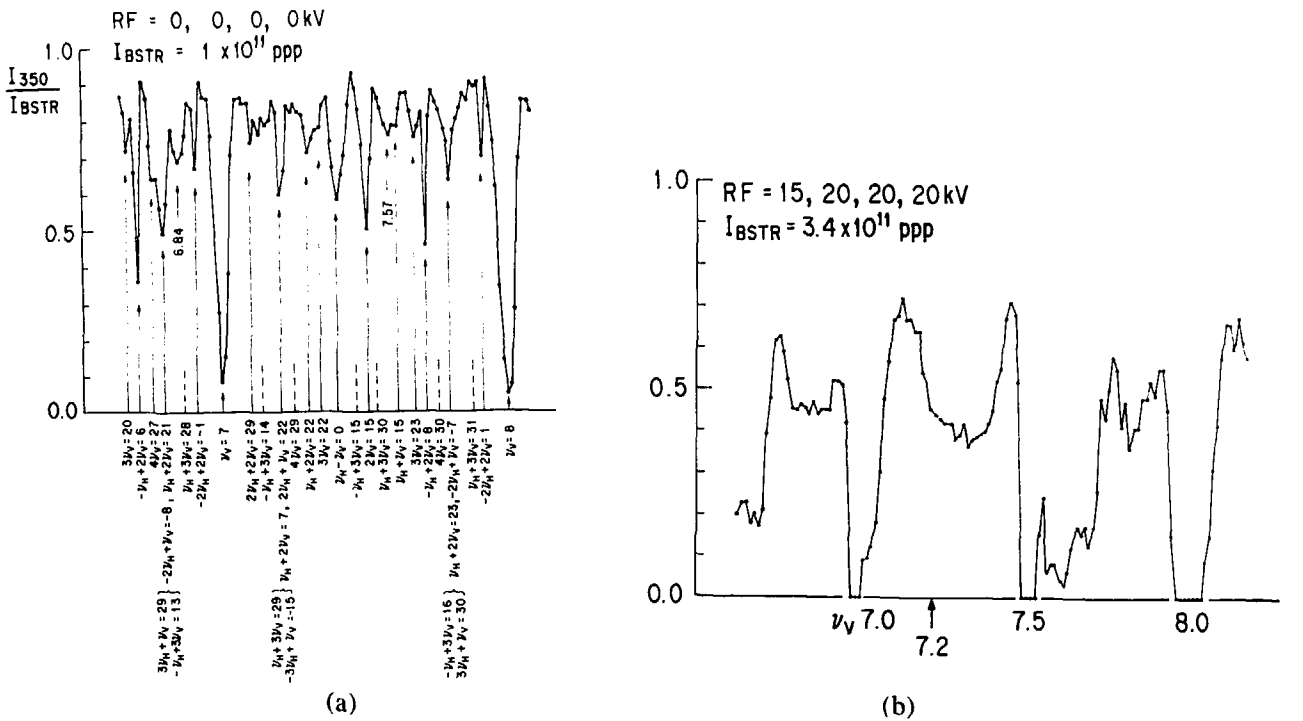

Fig.22 Resonance lines along $\nu_H = 7.4$ at the injection period. The vertical axis is the ratio of the surviving intensity at 350 ms after injection. The horizontal axis is the vertical tune measured by the tune meter with a low intensity bunched beam. The black points represent the measured points. Two results are (a) low intensity coasting beam, (b) high intensity bunched beam. Resonance lines up to the forth order are assigned to (a).

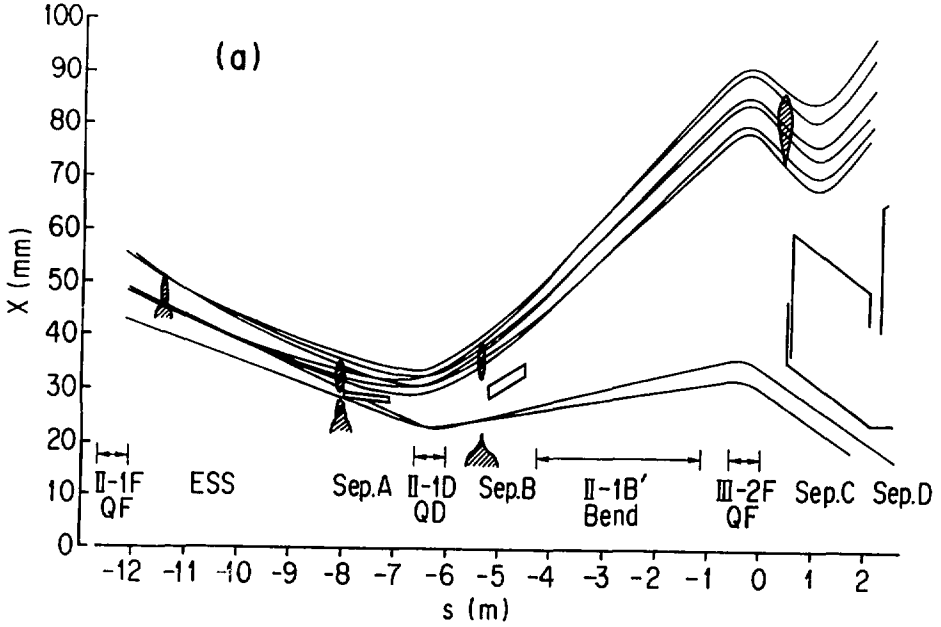

Fig.23 Beam size and trajectories of EP1 extracted beam.

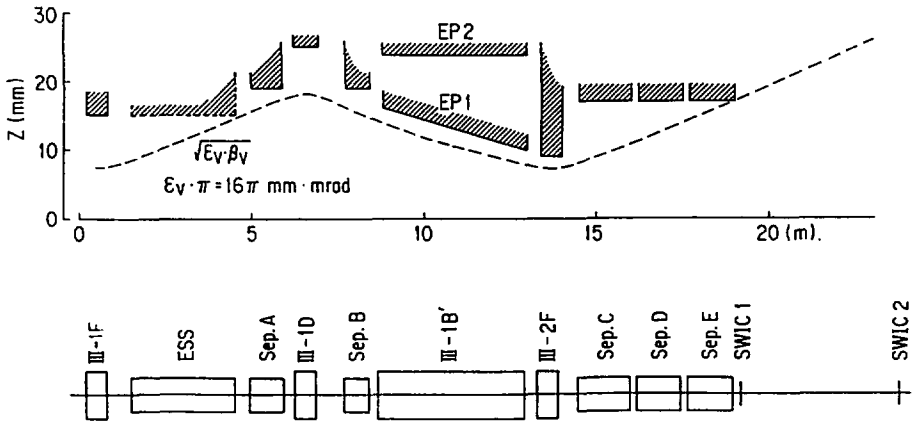

Fig.24 Vertical aperture for the extracted beam from ESS to the exit of the last septum (Septum E).